High Permeability and Low Loss Ni-Fe Composite Material for High-Frequency Applications

著者	寺本　章伸
journal or publication title	IEEE Transactions on Magnetics
volume	44
number	9
page range	2100-2106
year	2008
URL	http://hdl.handle.net/10097/47998

doi: 10.1109/TMAG.2008.2001073

High Permeability and Low Loss Ni–Fe Composite Material for High-Frequency Applications

Yasushi Shirakata[1,2], Nobuhiro Hidaka[1,3], Masayuki Ishitsuka[3], Akinobu Teramoto[1], and Tadahiro Ohmi[1], *Fellow, IEEE*

[1]New Industry Creation Hatchery Center, Tohoku University, Sendai 980-8679, Japan
[2]Research and Development Division, Yokowo Co., Ltd., Tokyo 114-8515, Japan
[3]Advanced Materials Research Laboratory, Sumitomo Osaka Cement Co., Ltd., Chiba 274-8601, Japan

A magnetic material with high permeability and low loss characteristics at high frequency is required for miniaturizing electronic components such as antennas. The key factors to keeping low magnetic loss are a high magnetic resonance frequency and the suppression of the eddy currents. We have fabricated a low-loss magnetic composite material by dispersing $Ni_{78}Fe_{22}$ (permalloy) fine flakes in polymers; the thickness of the flakes was less than skin depth. The magnetic loss decreased with increased stirring time, and the minimum value occurred when the agglomerated particles decreased and most of the particles were deformed into flakes. Moreover, $Zn_5Ni_{75}Fe_{20}$ composite material indicated high permeability when the flakes were oriented in the direction of sheets. The effect of wavelength shortening by permeability enhancement and the low loss characteristic were confirmed by experimental results of a rod antenna loaded with the developed magnetic composite material.

***Index Terms*—Antennas, high frequency, magnetic loss, permalloy, permeability.**

I. INTRODUCTION

THE rapid growth of multifunctioning and the downsizing of portable communication devices, such as cellular phones, demands a further miniaturization and a high density mounting of electronic components. This is particularly true for antennas, where the demand for miniaturizing has risen for internal antennas inside a portable terminal. Some techniques are known for miniaturizing antennas. For instance, adding a matching circuit, changing the route of the currents, loading dielectric and magnetic material, and so on. The length of the electromagnetic wave propagating inside the material is given by

$$\lambda_g = \frac{\lambda_0}{\sqrt{\epsilon_r \mu_r}} \tag{1}$$

where λ_g, λ_0, ϵ_r, and μ_r are wavelength in the material, wavelength in vacuum, relative permittivity, and relative permeability of material, respectively. Hence, the miniaturization of an antenna becomes possible by loading material which has large value of ϵ_r and μ_r[1].

Furthermore, the impedance of the material is given by

$$Z_m = Z_0\sqrt{\frac{\mu_r}{\epsilon_r}} \tag{2}$$

where Z_m and Z_0 are the impedance of the material and vacuum, respectively. By loading magnetic material and making almost equal values of ϵ_r and μ_r, the improvement of the antenna properties can be expected, as the impedance of the antenna matches to the impedance of free air [2].

Recently, in Japan, cellular phones have been required to have reception functions of UHF and FM bands, therefore a material which has a large effect on wavelength shortening is desired. Though the dielectric material is generally used for miniaturizing antennas such as ceramic patch antennas, there is the problem that the bandwidth narrows because very high permittivity is demanded. To solve such problems, an antenna loaded with magnetic materials has been researched, and for instance, the miniaturized Planar Inverted-F Antenna (PIFA) and Meander Line Antenna (MLA) were reported [3]–[5].

Ferrite is a magnetic material that is known to have excellent properties at high frequency. However, there is a relational expression between the initial permeability μ_i and the resonant frequency f_r, which is called Snoek's limit [6], [7] described as

$$\mu_i \cdot f_r = \frac{\gamma}{3\pi} M_s \tag{3}$$

where γ is the gyromagnetic ratio, and M_s is the saturation magnetization. Having high saturation magnetization is important for high-frequency applications [8], and the ferrite is an inadequate material in the gigahertz band because of its small saturation magnetization.

Metallic magnetic material has comparatively larger saturation magnetization than the ferrite, hence the resonant frequency can be raised. However, the eddy current, due to its high electric conductivity, causes an increase in loss and a decrease in permeability at high frequency. Reducing the thickness of the magnetic material to less than skin depth is effective in decreasing the eddy current. The skin depth d is described as

$$d = \sqrt{\frac{2}{\omega\mu\sigma}} \tag{4}$$

where ω, μ, and σ are the angular frequency, the permeability, and the electric conductivity, respectively. Thus, the skin depth becomes several micrometers at 1 GHz.

Digital Object Identifier 10.1109/TMAG.2008.2001073

The effective permeability also decreases by the demagnetization field depending on the shape of the magnetic material. On the inside of the magnetic material, the magnetizing force H is determined by the relation

$$H = H_0 - NJ \tag{5}$$

where H_0, N, and J are the external applied field, the demagnetizing factor, and the magnetization, respectively. N depends on the aspect ratio of the material. Though N is equal to $1/3$ for spherical particles, in all other cases such as needle-shaped, flake-shaped, and so on, N is smaller than $1/3$ in a long axis direction [9]. It has been reported that an aspect ratio of 10 or more is preferable to increase permeability in the microwave range [10].

Based on these theoretical backgrounds, desirable properties of magnetic material at high frequency can be obtained by dispersing flake-shaped metallic magnetic particles in polymers, with the thickness of the particles being less than skin depth. In the past, high-frequency magnetic properties of the composite materials that are made of flat metallic particle such as Fe–Si–Al and Fe have been reported [11], [12]. However, these materials indicated high permeability and high loss at high frequency, hence they are assumed to be used for electromagnetic interference (EMI) suppression.

The purpose of this study is to fabricate a magnetic material that indicates low loss characteristics in spite of high permeability. The key points to suppress the eddy currents are to use fine particles that are smaller than skin depth and to disperse them uniformly in polymers. The raw material particles should be as fine as possible, because they become easily coarse by rolling and cohesion when spherical particles are deformed into flakes. Less than 0.2 μm of the diameter of the particle is preferable according to (4). The techniques of crushing agglomerated particles and preventing re-agglomeration are also important since the fine particles tend to agglomerate.

The magnetic properties of a composite material filled with metallic magnetic particles are inferior in comparison with that of bulk, since the magnetism of each of the metallic particles acts on a the surrounding space separately. To obtain a high permeability, the raw material particles should have a small coercive force H_c and a large saturation magnetization M_s. Ni–Fe alloy ($Ni_{78}Fe_{22}$, permalloy) is known to have an excellent soft magnetic property due to its small magnetic anisotropy, low magnetostriction, and high dc permeability. However, the diameter of the Ni–Fe alloy particle, which is obtained by a general manufacturing method called the atomize method, is usually over 1 μm, hence it is unsuitable to decrease the eddy current at 1 GHz. Although the vapor phase reduction method is known as a process of preparing comparatively small particles, due to its high temperature processing, particles are easily fused by contact, thus it is difficult to prevent a large particle being generated.

This paper describes the magnetic properties of our developed composite material, which indicates high permeability and low loss characteristics at high frequency. The composite material consists of flakes dispersed in polymers. The 0.15 μm

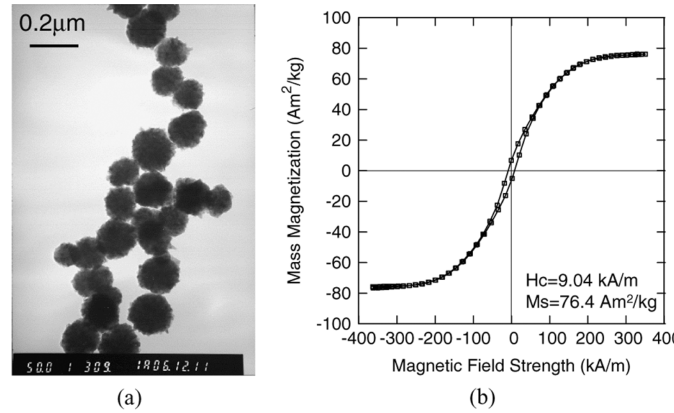

Fig. 1. (a) TEM image and (b) hysteresis loop of Ni–Fe particles measured at room temperature.

Ni–Fe alloy as a raw material particle was prepared by the liquid phase reduction method. In addition, the characteristics of a rod antenna loaded with the fabricated composite material are described.

II. Experimental Details

A. Characteristics of the Raw Material

Fine particles of Ni–Fe ($Ni_{78}Fe_{22}$) alloy were prepared by reducing nickel chloride hexahydrate ($NiCl_2 \cdot 6H_2O$) and iron chloride tetrahydrate ($FeCl_3 \cdot 4H_2O$) in an aqueous solution. Similarly, fine particles of Zn–Ni–Fe ($Zn_5Ni_{75}Fe_{20}$) alloy were prepared by the addition of zinc nitrate hexahydrate ($Zn(NO_3)_2 \cdot 6H_2O$) to the aqueous solution. Figs. 1(a) and 2(a) show the images of Ni–Fe fine particles and Zn–Ni–Fe fine particles, respectively, observed by a Hitachi H-800 transmission electron microscope (TEM). The particles were spherical and the median diameter was 0.15 μm for Ni–Fe and 0.25 μm for Zn–Ni–Fe. Hysteresis loops measured by a Hayama OP-01 vibrating sample magnetometer (VSM) are shown in Figs. 1(b) and 2(b). The coercive force H_c and the saturation magnetization M_s was 9.04 kA/m and 76.4 $A \cdot m^2$/kg for Ni–Fe particle and 4.73 kA/m and 73.7 $A \cdot m^2$/kg for Zn–Ni–Fe particle, respectively. Though Zn–Ni–Fe became slightly small M_s because of the addition of nonmagnetic Zn atoms, H_c was improved and showed an excellent magnetic property compared with Ni–Fe.

B. Preparation of Magnetic Composite Material

The preparation procedure of the magnetic composite material is as follows. The raw material particles, and the zirconia balls which have diameters of 200 μm as grinding media, were put in the solvent with the surfactant. When the slurry in the high-speed rotation-revolution mixer was stirred at an acceleration of approximately 3900 m/s^2, the agglomerated particles were crushed in a short time. Also the particles were deformed into flakes with 2 μm length and 0.2 μm thickness. Flakes were mixed with thermosetting polymer so that the volume content might become 38%. A film of approximately 60 μm thickness was fabricated by the doctorblade method and dried at 323 K in the atmosphere. The composite material of approximately 0.3 to 0.6 mm thickness was prepared by laminating films, which

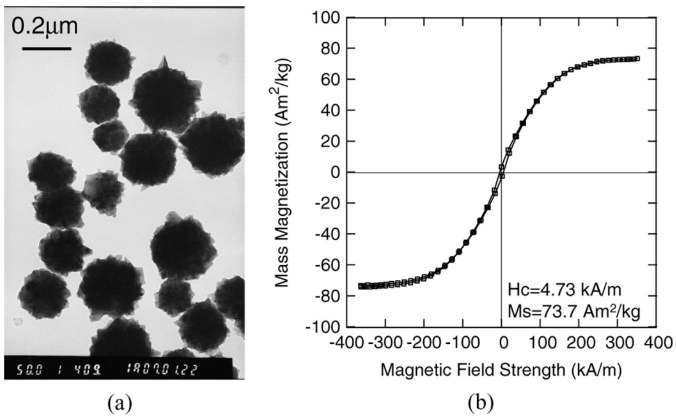

Fig. 2. (a) TEM image and (b) hysteresis loop of Zn–Ni–Fe particles measured at room temperature.

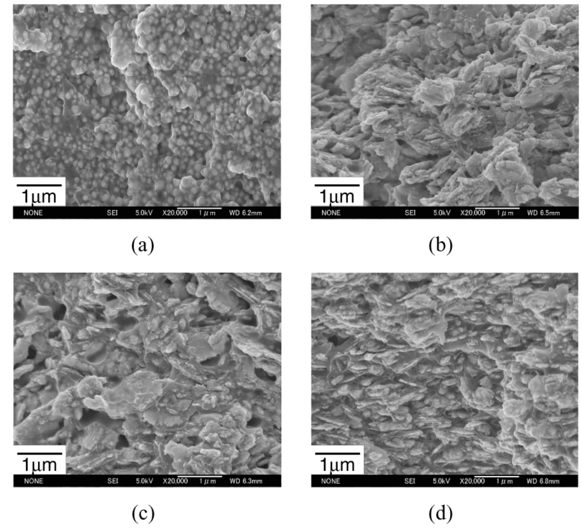

Fig. 3. Cross-sectional SEM images of Ni–Fe composite materials for different stirring times. (a) 0 min, (b) 30 min, (c) 50 min, and (d) 80 min.

were hot-pressed at 433 K under uniaxial pressure of 0.1 MPa for 40 min in 0.01 MPa vacuum atmosphere.

C. Measurement of the Material

The microstructure of the fabricated composite material was observed by a JEOL JSM-6700F scanning electron microscope (SEM). The permeability characteristic of a direction parallel to the sheet was measured by an Agilent 8791ES vector network analyzer using the parallel line method [13]. The permittivity characteristic of a direction perpendicular to the sheet was measured by a Hewlett-Packard 4291A impedance analyzer using the parallel plate capacitor method.

III. Results and Discussion

A. Characteristics of the Ni–Fe Composite Material

Fig. 3 shows the microstructures of Ni–Fe composite material for different stirring times. As shown in the figure, particles were crushed and deformed into flakes as the stirring time increased. The permeability characteristics are shown in Fig. 4. At the stirring time of 0 (i.e., nonprocessing), imaginary part of the complex permeability μ'' has two peaks at approximately 0.7 and 4 GHz, and high loss was seen in a broad frequency range [Fig. 4(a)]. Though the peak on a higher frequency region seems to be caused by the magnetic resonance, the one on a lower frequency region depends on the size of the particles. As the stirring time increased, a peak on a lower frequency region shifted to the higher region. As a result, μ'' at 1 GHz became the minimum value by stirring for 30 min [Fig. 4(d)]. The obtained permeability was $\mu' = 5, \mu'' = 0.4$, and the calculated magnetic loss factor $\tan\delta\mu$ was 0.08. In addition, the obtained permittivity was $\epsilon' = 13$ and the calculated dielectric loss factor $\tan\delta\epsilon$ was 0.04. As compared with the composite material used for the EMI suppression having $\tan\delta\mu$ of 0.5 to 1, the fabricated material showed quite low loss characteristics. When the stirring continued further, μ'' gradually increased again [Fig. 4(e) and (f)]. We consider that the reason for this is that the size and shape became heterogeneous because particles repeated destruction and cohesion.

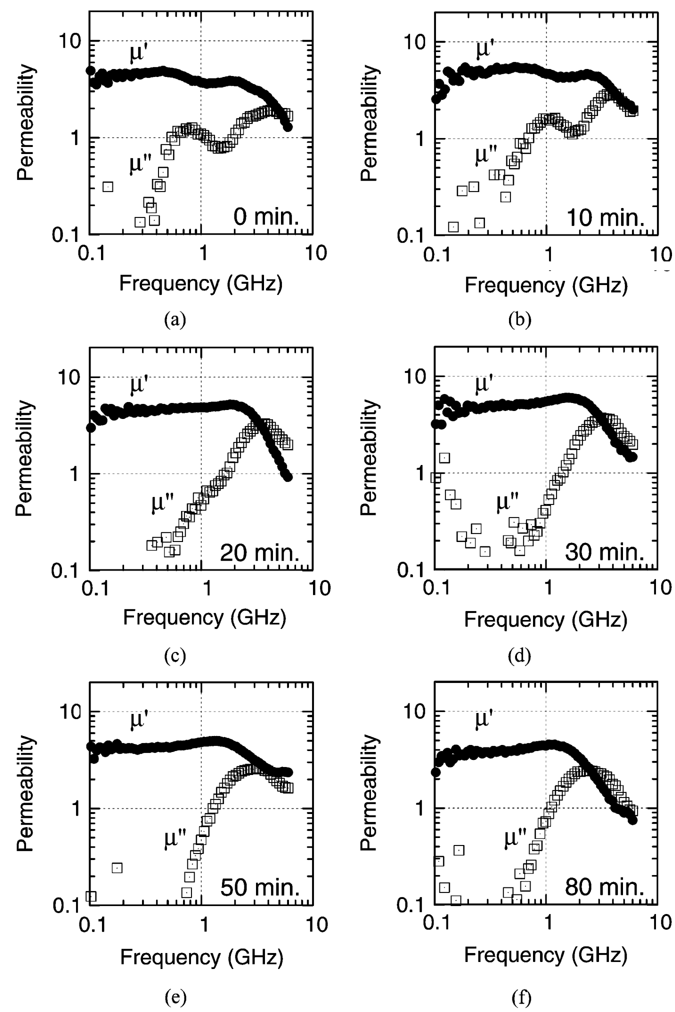

Fig. 4. Permeability characteristics of Ni–Fe composite materials for different stirring times. (a) 0 min, (b) 10 min, (c) 20 min, (d) 30 min, (e) 50 min, and (f) 80 min.

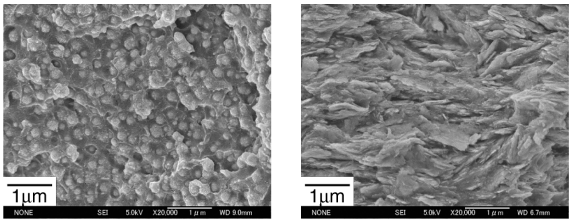

(a) (b)

Fig. 5. Cross-sectional SEM images of Zn–Ni–Fe composite materials for different stirring times. (a) 0 min and (b) 30 min.

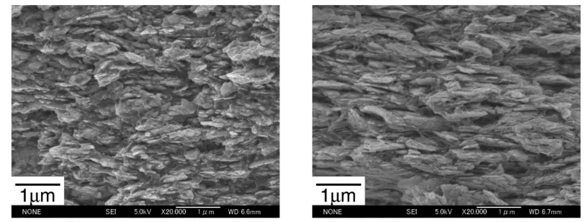

(a) (b)

Fig. 7. Cross-sectional SEM images of composite materials consists of (a) oriented Ni–Fe particles and (b) oriented Zn–Ni–Fe particles.

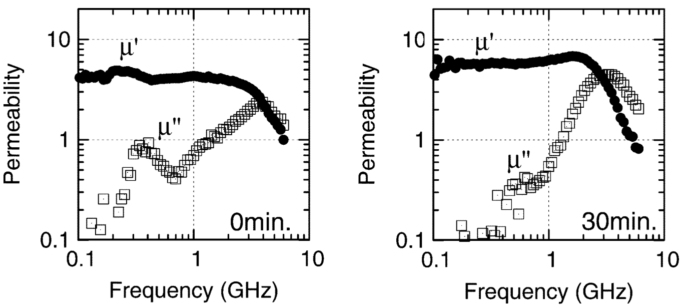

(a) (b)

Fig. 6. Permeability characteristics of Zn–Ni–Fe composite materials for different stirring times. (a) 0 min and (b) 30 min.

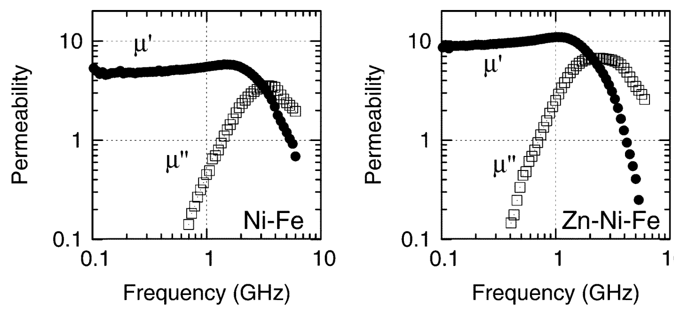

(a) (b)

Fig. 8. Permeability characteristics of composite materials consists of (a) oriented Ni–Fe particles and (b) oriented Zn–Ni–Fe particles.

B. Characteristics of the Zn–Ni–Fe Composite Material

The Zn–Ni–Fe composite material was prepared in the same process as the Ni–Fe composite material. The microstructures of the material are shown in Fig. 5. As shown in the figure, the particle was crushed and deformed into flakes by stirring. Permeability characteristics of the Zn–Ni–Fe composite material are shown in Fig. 6. At the stirring time of 0 (i.e., nonprocessing), μ'' has two peaks at approximately 0.4 and 4 GHz [Fig. 6(a)]. As well as the Ni–Fe alloy material, the decrease of μ'' was seen along with the stirring and as a result, μ'' at 1 GHz became the minimum value by stirring for 30 min [Fig. 6(b)]. For this material, the obtained permeability was $\mu' = 6, \mu'' = 0.6$, and calculated $\tan\delta\mu$ was 0.1. In addition, the obtained permittivity was $\epsilon' = 13$ and calculated $\tan\delta\epsilon$ was 0.05. This material also shows sufficiently low loss for high-frequency application usage.

C. Permeability Enhancement of Zn–Ni–Fe Composite Material Gained by Oriented Particles

We impressed the external magnetic field to the film fabricated by the doctorblade method while being dried, thus the long axis of flakes became parallel to the direction of the sheets (Fig. 7). The permeability enhancement of the Ni–Fe composite material was slight [Fig. 8(a)]. By contrast, the Zn–Ni–Fe composite material indicated great enhancement of permeability which are $\mu' = 11, \mu'' = 2.5$, and $\tan\delta\mu = 0.22$ at 1 GHz [Fig. 8(b)]. To investigate the reason why the permeability increased only in the Zn–Ni–Fe composite material, the crystal structure of the particles in the composite material that was stirred for 30 min was evaluated by PANalytical X'Pert PRO X-ray diffraction (XRD) patterns. Fig. 9 shows the XRD patterns of $\theta - 2\theta$ measured at different tilt angle ψ. The patterns show that both the Ni–Fe alloy and the Zn–Ni–Fe alloy had face-centered cubic (fcc) structures and no other products were seen in the crystals. As for the Ni–Fe composite material, their peaks intensity are almost constant for ψ changing whether its particles are oriented or not [Fig. 9(a) and (b)]. As for the Zn–Ni–Fe composite material, the peaks intensity did not change when the particles were not oriented [Fig. 9(c)]. In contrast, when they were oriented, (111) and (200) diffraction peaks intensity increased significantly, and (220) peak intensity decreased when ψ was 45° [Fig. 9(d)]. These results suggest that the crystal structure was oriented along a particular direction in Zn–Ni–Fe. This implies that plastic deformation by mechanical stress occurred in a specific direction of the crystal, since malleability increased by the effect of the Zn. That is, when the particle is deformed into flakes, the axis of easy magnetization turns to the direction of the long axis of the flake. Permeability increased to a large value of approximately 10 because the axis of an easy magnetization agreed with the direction of the magnetic field and also the demagnetization factor N has decreased by orientating the particle. By contrast, permeability was only approximately 6 when the particle was not oriented or was made without addition of Zn, since an arrangement of flakes or a crystal structure becomes random and the axis of easy magnetization does not agree with a constant direction.

D. Evaluation of Antenna Loaded With Magnetic Composite Material

To confirm the effect of magnetic properties in high frequency applications, the characteristics of a rod antenna loaded with the

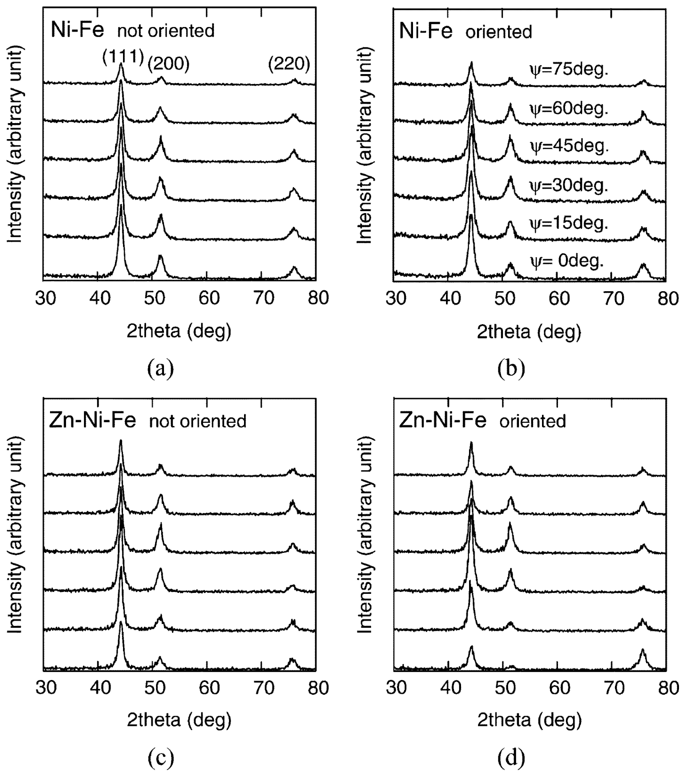

Fig. 9. X-ray diffraction patterns of composite materials stirred for 30 min recorded at different tilt angle ψ: (a) nonoriented Ni–Fe particles, (b) oriented Ni–Fe particles, (c) nonoriented Zn–Ni–Fe particles, and (d) oriented Zn–Ni–Fe particles.

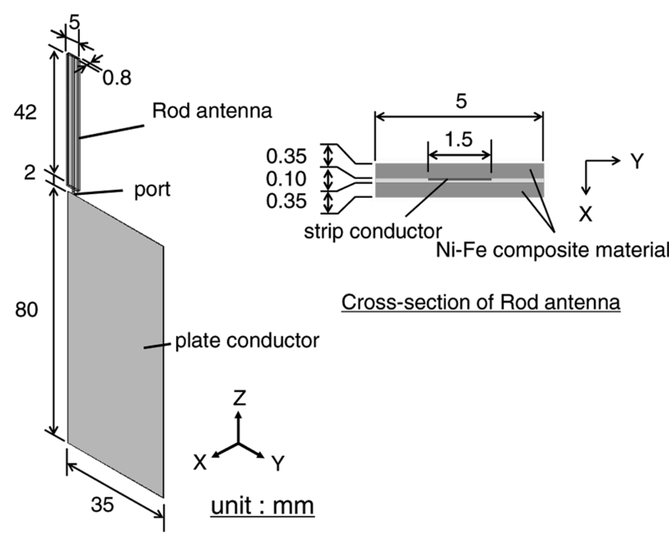

Fig. 10. Schematic configuration and cross-sectional view of the antenna.

fabricated composite material was investigated. The rod antenna is a very basic structure, which simplifies the comparison between the experimental result and the simulation result. Fig. 10 shows the configuration of the evaluated antenna. The magnetic loaded rod antenna consisted of 44 mm × 1.5 mm × 0.05 mm strip conductor and 2 of 42 mm × 5 mm × 0.35 mm magnetic composite materials which were stuck together from both sides of the strip conductor with 0.1 mm thickness double-faced adhesive tape. The magnetic composite materials were made of

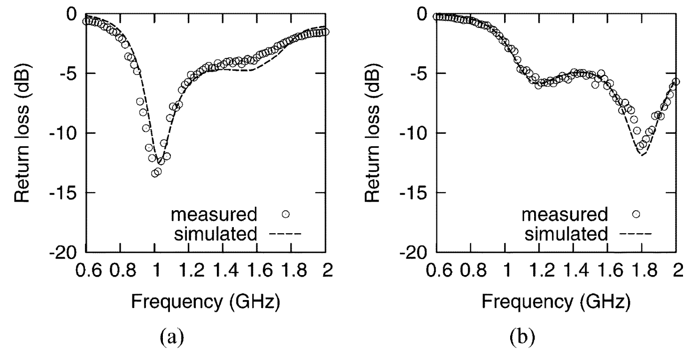

Fig. 11. Return loss characteristics of the antenna: (a) loaded with Ni–Fe composite material (stirred for 30 min and not oriented) and (b) without material.

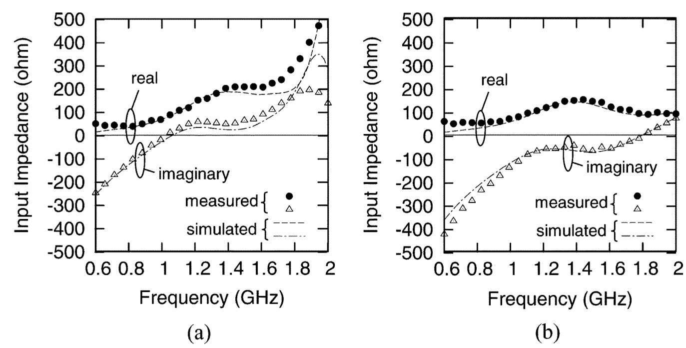

Fig. 12. Input impedance characteristics of the antenna: (a) loaded with Ni–Fe composite material (stirred for 30 min and not oriented) and (b) without material.

38 vol% Ni–Fe particles which had been stirred for 30 min and not oriented. The rod antenna was connected to a 35 mm × 80 mm × 0.1 mm plate conductor.

The simulation was performed by the electromagnetic full-wave simulator Ansoft High Frequency Structure Simulator (HFSS) Ver. 9.1.2 which is able to set the value of ϵ_r, μ_r, and $\tan\delta$, separately. The size of the air box was 500 mm × 500 mm × 500 mm and the boundary was set to nonreflective (radiation) layer. The parameters of the magnetic composite material were set to $\epsilon_r = 13, \tan\delta\epsilon = 0.04, \mu_r = 5$, and $\tan\delta\mu = 0.1$. These parameters are assumed to take definite value that does not depend on frequency.

Return loss and input impedance characteristics of the antenna were measured by an Agilent Technologies E8364B PNA network analyzer. Fig. 11(a) and (b) show the return loss characteristics of the rod antenna with the magnetic composite material and without the material (i.e., an usual rod antenna), respectively. We can see two resonance modes because this antenna is a kind of dipole antenna which has asymmetric arms. The higher resonance mode depends on the length of the rod structure (44 mm), and the lower resonance mode depends on the length of the entire antenna (124 mm). Fig. 12(a) and (b) show the input impedance characteristics of the antenna with the magnetic composite material and without the material, respectively. The imaginary part of impedance increased by approximately 150 ohms by loading the magnetic materials, and as a result, the lower resonance mode became superior so that the resonance frequency of the antenna shifted from 1.8 to 1.0 GHz. Fig. 13

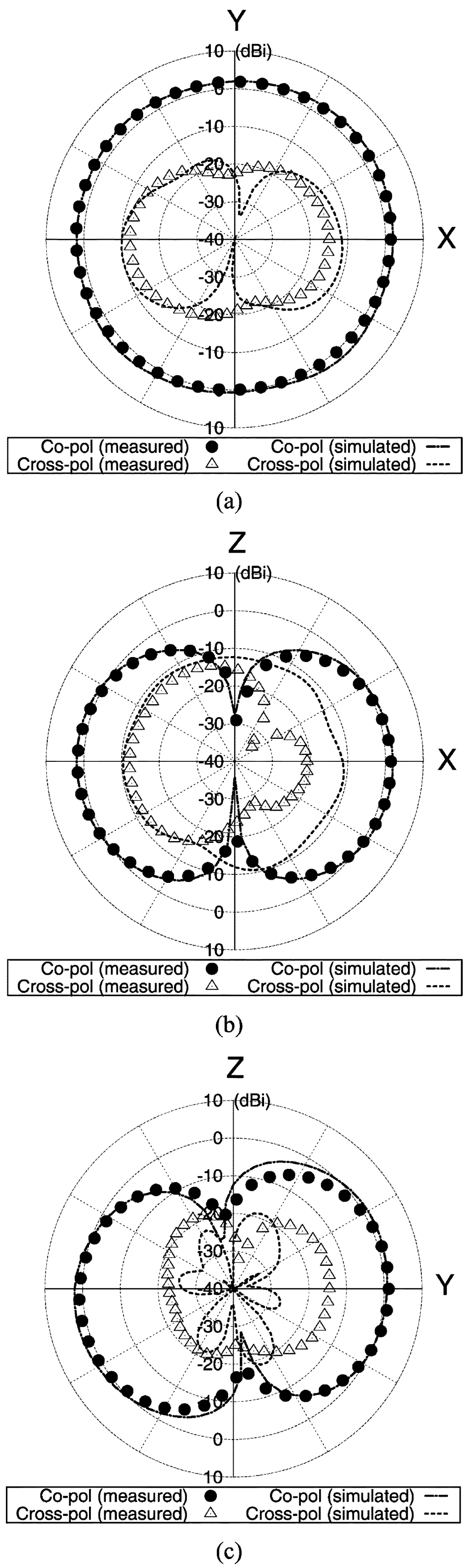

Fig. 13. Radiation patterns measured at 1.0 GHz for the antenna loaded with the Ni–Fe composite material (stirred for 30 min and not oriented). (a) X–Y plane, (b) X–Z plane, and (c) Y–Z plane.

shows the radiation patterns at 1.0 GHz. The experimental results agree well with the simulation results and the radiation efficiency calculated from the obtained gain was 86.3%, hence the influence of the material loss was hardly seen.

As a result, the developed composite material indicates high permeability and low magnetic loss properties in the gigahertz band, therefore, we are able to conclude that this material is very useful for high-frequency applications.

IV. Conclusion

We presented the magnetic properties of developed magnetic composite materials with high permeability and low loss characteristics at high frequency. The composite material consists of $Ni_{78}Fe_{22}$ or $Zn_5Ni_{75}Fe_{20}$ fine flakes dispersed in polymers. The raw material particles with a median diameter of 0.15 μm are prepared by the liquid phase reduction method. Magnetic loss decreases with an increase of the stirring time, and the minimum value can be obtained when the agglomerated particles decrease and most particles are deformed into flakes. Moreover, the Zn–Ni–Fe composite material indicates high permeability when the flakes are oriented in the direction of the sheets. The effect of wavelength shortening and low loss characteristics are verified by the experimental results of a rod antenna loaded with developed magnetic composite material.

In conclusion, the possibility and the feasibility of miniaturizing electronic components by loading the developed magnetic composite material were confirmed. We propose to make and study further high permeability and low loss materials that can be applied to built-in terminal antennas.

Acknowledgment

This work was supported in part by Sendai Knowledge Cluster Initiative by the Ministry of Education, Culture, Sports, Science and Technology (MEXT), Japan.

References

[1] R. C. Hansen and M. Bruke, “Antennas with magneto-dielectrics,” *Microw. Opt. Technol. Lett.*, vol. 26, no. 2, pp. 75–78, July 2000.

[2] L. B. Kong, Z. W. Li, G. Q. Lin, and Y. B. Gan, “Ni-Zn ferrites composites with almost equal values of permeability and permittivity for low-frequency antenna design,” *IEEE Trans. Magn.*, vol. 43, no. 1, pp. 6–10, Jan. 2007.

[3] T. Tanaka, S. Hayashida, K. Imamura, H. Morishita, and Y. Koyanagi, “A study on miniaturization of a handset antenna utilizing magnetic materials,” in *Proc. Joint Conf. 10th Asia-Pacific Conf. Commun. and 5th Int. Symp. Multi-Dimensional Mobile Commun. (APCC&MDMC)*, Beijing, China, Aug. 2004, vol. 2, pp. 665–669.

[4] Y. Mano and S. Bae, “A small meander antenna by magneto-dielectric material,” in *Proc. IEEE Int. Symp. Microwave, Antenna, Propag. and EMC Tech. Wireless Commun. (MAPE)*, Beijing, China, Aug. 2005, vol. 1, pp. 63–66.

[5] K. S. Min and T. V. Hong, “Miniaturization of antenna using magneto-dielectric materials,” in *Proc. 2006 Asia-Pacific Conf. Commun. (APCC)*, Busan, Korea, Aug. 2006, pp. 1–5.

[6] J. L. Snoek, “Dispersion and absorption in magnetic ferrites at frequencies above one Mc/s,” *Physica*, vol. 14, no. 4, pp. 207–217, May 1948.

[7] R. Lebourgeois, C. L. Fur, M. Labeyrie, M. Pate, and J. P. Ganne, “Permeability mechanisms in high frequency polycrystalline ferrites,” *J. Magn. Magn. Mater.*, vol. 160, pp. 329–332, Jul. 1996.

[8] O. Acher and A. L. Adenot, “Bounds on the dynamic properties of magnetic materials,” *Phys. Rev. B*, vol. 62, no. 17, pp. 11324–11327, Nov. 2000.

[9] J. A. Osborn, “Demagnetizing factors of the general ellipsoid,” *Phys. Rev.*, vol. 67, no. 11–12, pp. 351–357, Jun. 1945.

[10] R. Walser, W. Win, and P. Valanju, “Shape-optimized ferromagnetic particles with maximum theoretical microwave susceptibility,” *IEEE Trans. Magn.*, vol. 34, no. 4, pp. 1390–1392, Jul. 1998.

[11] S. Yoshida, M. Sato, E. Sugawara, and Y. Shimada, "Permeability and electromagnetic-interference characteristics of Fe-Si-Al alloy flakes-polymer composite," *J. Appl. Phys.*, vol. 85, no. 8, pp. 4636–4638, Apr. 1999.

[12] S. S. Kim, S. T. Kim, Y. C. Yoon, and K. S. Lee, "Magnetic, dielectric, and microwave absorbing properties of iron particles dispersed in rubber matrix in gigahertz frequencies," *J. Appl. Phys.*, vol. 97, no. 10, Jan. 2005.

[13] T. Kimura, M. Mitera, M. Terasaka, M. Nose, F. Matsumoto, H. Matsuki, H. Fujimori, and T. Masumoto, "System for measuring thin-film permeability by using a parallel line," *J. Magn. Soc. Jpn.*, vol. 17, no. 2, pp. 497–502, 1993.

Manuscript received March 24, 2008; revised May 30, 2008. Published August 20, 2008 (projected). Corresponding author: Y. Shirakata (e-mail: shirakata@yokowo.co.jp).

Yasushi Shirakata (M'03) was born in Ibaraki, Japan, in 1970. He received the B.S. and M.S. degrees in applied physics from Waseda University, Tokyo, Japan, in 1994 and 1996, respectively.

From 1996 to 2001, he was with Tokimec Inc., Tokyo, Japan, where he was engaged in the development of microwave devices. In 2002, he moved to Yokowo Co., Ltd., Tokyo, Japan, where he was engaged in research and development of microwave antennas. From 2004 to 2008, he was a Visiting Researcher at the New Industry Creation Hatchery Center, Tohoku University, Sendai, Japan. He is currently engaged in research and development of magnetic materials for microwave applications.

Mr. Shirakata is a member of the Institute of Electronics, Information and Communication Engineers of Japan and the Magnetics Society of Japan.

Nobuhiro Hidaka was born in Kagoshima, Japan, on October 27, 1978. He received the B.S., M.S., and Ph.D. degrees in material engineering from Kagoshima University, Kagoshima, Japan, in 2002, 2003, and 2006, respectively.

He joined the Sumitomo Osaka Cement Corporation, Tokyo, Japan, in 2006. From 2006 to 2008, he was a Visiting Researcher at the New Industry Creation Hatchery Center, Tohoku University, Sendai, Japan. He is currently engaged in the research and development of magnetic materials.

Masayuki Ishitsuka was born in Ibaraki, Japan, on December 19, 1962. He received the B.S., M.S., and Ph.D. degrees in material chemistry from Tohoku University, Sendai, Japan, in 1985, 1987, and 1990, respectively.

He joined the Sumitomo Osaka Cement Corporation, Tokyo, Japan, in 1990. He is currently engaged in the research and development of magnetic materials.

Akinobu Teramoto (M'02) received the B.S. and M.S. degrees in electronic engineering and the Ph.D. degree in electrical engineering from Tohoku University, Sendai, Japan, in 1990, 1992, and 2001, respectively.

From 1992 to 2002, he worked at Mitsubishi Electric Corporation, Hyogo, Japan, where he has been engaged in the research and development of thin silicon dioxide films. In 2002, he moved to Tohoku University and he is currently an Associate Professor at the New Industry Creation Hatchery Center. He is currently engaged in an advanced semiconductor device technologies and process technologies, such as SOI MOS transistors, accumulation-mode transistors, variation and noise of transistors, high-quality low-temperature oxidation, nitridation, and CVD process using microwave-exited high-density plasma.

Dr. Teramoto is a member of the Electrochemical Society, the Japan Institute of Electronics Packaging, the Institute of Electronics, Information and Communication Engineers of Japan, and the Japan Society of Applied Physics.

Tadahiro Ohmi (M'81–SM'01–F'03) received the B.S., M.S., and Ph.D. degrees in electrical engineering from Tokyo Institute of Technology, Tokyo, Japan, in 1961, 1963, and 1966, respectively.

Prior to 1972, he served as a Research Associate in the Department of Electronics, Tokyo Institute of Technology, where he worked on Gunn diodes such as velocity overshoot phenomena, multivalley diffusion and frequency limitation of negative differential mobility due to an electron transfer in the multi-valleys, high-field transport in semiconductor such as unified theory of space-charge dynamics in negative differential mobility materials, Bloch-oscillation-induced, negative mobility and Bloch oscillators, and dynamics in injection lasers. In 1972, he moved to Tohoku University, Sendai, Japan, where he is currently a Professor at the New Industry Creation Hatchery Center. He is engaged in researches on high-performance ULSI such as ultrahigh-speed ULSI based on gas-isolated-interconnect metal-substrate SOI technology, base store image sensor (BASIS) and high-speed flat-panel display, and advanced semiconductor process technologies such as low kinetic-energy particle bombardment processes including high-quality oxidation, high-quality metallization, very-low-temperature Si epitaxy, and crystallinity-controlled film growth technologies from single-crystal, grain-size-controlled polysilicon and amorphous highly selective CVD, highly selective RIE, and high-quality ion implantation with low-temperature annealing capability based on ultraclean technology concept supported by newly developed ultraclean gas supply system, ultrahigh vacuum-compatible reaction chamber with self-cleaning function, and ultraclean wafer surface cleaning technology. His research activities are summarized by the publication of over 800 original papers and the application of 800 patents.

Dr. Ohmi serves as the President of the Institute of Basic Semiconductor Technology-Development (Ultra Clean Society). He is a Fellow of the Institute of Electricity, Information and Communication Engineers of Japan. He is a member of the Institute of Electronics of Japan, the Japan Society of Applied physics, and the Electrochemical Society. He received the Ichimura Award in 1979, the Inoue Harushige Award in 1989, the Ichimura Prizes in Industry-Meritorious Achievement Prize in 1990, the Okouchi Memorial Technology Prize in 1991, the Minister of State for Science and Technology Award for the Promotion of Invention (the Invention Prize) in 1993, the IEICE Achievement Award in 1997, the Okouchi Memorial Technology Prize in 1999, the Werner Kern Award in 2001, the ECS Electronics Division Award, the Medal with Purple Ribbon from Government of Japan and the Best Collaboration Award (the Prime Minister's Award) in 2003.